

Graphene-type Sheets of Nb_{1-x}W_xS₂: Synthesis and *in situ* Functionalization

Faegheh Hoshyargar,^a Jugal Kishore Sahoo,^a Muhammad Nawaz Tahir,^a Aswani Yella,^a Michael Dietzsch,^a Filipe Natalio,^a Robert Branscheid,^b Ute Kolb,^b Martin Panthöfer^a and Wolfgang Tremel,^{*a}

Received (in XXX, XXX) Xth XXXXXXXXX 200X, Accepted Xth XXXXXXXXX 200X

First published on the web Xth XXXXXXXXX 200X

DOI: 10.1039/b000000x

Supporting Information

Dynamic Light Scattering:

I. Light Scattering Setup. The DLS setup consisted of an ALV-5000 correlator, equipped with an ALV/SP125 goniometer and avalanche photodiode detector. An argon ion laser ($\lambda = 514.5$ nm, $P = 500$ mW output power) served as a coherent light source. Measurements were carried out at 30, 50, 70, 90, 110, 130 and 150° and at a temperature of 20°C. 5 runs were recorded at every angle to increase the signal to noise ratio.

II. Dynamic Coefficient Measurements for the Fresh Sample. The field correlation $g_1(\tau)$ could be well fitted with the cumulant series expansion

$$g_1(\tau) = a + b \cdot \exp\left(-\frac{\tau}{c}\right) \cdot [1 + d \cdot \tau^2]$$

With a representing the baseline (which was subtracted before fitting) and b representing the amplitude. C , being the decay time of the correlation function, yields the z-average diffusion coefficient $\langle D \rangle_{z,app} = 1/c \cdot q^2$ of the particles, with q as the scattering vector $q = 4\pi n \sin(\theta/2)/\lambda_0$. In cases of a polydisperse sample consisting of larger particles ($d > \lambda/20$), a measurement performed at a finite angle only yields an apparent diffusion coefficient $\langle D \rangle_{z,app}$, which increases with the scattering angle due to the contribution of the particle form factor. The true z-average $\langle D \rangle_z$ can then be obtained by extrapolating towards $\theta = q^2 = 0$.

Finally, the second cumulant d is a quantitative measure for the width of the diffusion coefficient distribution and hence for the dispersity of the sample

$$\sigma^2(D) = (\Delta D)^2 = \langle D^2 \rangle - \langle D \rangle^2 = \frac{2d}{q^4}$$

By applying Stokes-law of diffusion, which assumes spherically shaped particles, the hydrodynamic radius can be obtained from the diffusion coefficient

$$\langle R_H \rangle = \frac{kT}{6\pi\eta\langle D \rangle}$$

Linear extrapolation to $\theta=q^2=0$ in Figure 5a yields a z-averaged diffusion coefficient of

$\langle D \rangle_z = 3.20 \times 10^{-8} \text{ cm}^2/\text{s}$ and a hydrodynamic radius of $R_H = 67 \text{ nm}$.

The second coefficient of the cumulant series expansion represents a quantitative measure for the dispersity of the sample. At 90° , a standard deviation of $\sigma(D) = 0.856 \times 10^{-8} \text{ cm}^2/\text{s}$ was obtained, which was used to plot the distribution curve, based on a standard deviation.

III. Diffusion Coefficient Measurements after 4 Weeks. From the same stock solution ($[\text{Nb}_{1-x}\text{W}_x\text{S}_2] = 0.05 \text{ mg/mL}$), a new sample was prepared ($[\text{NaCl}] = 10 \text{ mM}$, $[\text{Nb}_{1-x}\text{W}_x\text{S}_2] = 0.01 \text{ mg/mL}$) 4 weeks later shows the diffusion coefficients measured at different angles and via linear extrapolation a diffusion coefficient of $\langle D \rangle_z = 2.67 \cdot 10^{-8} \text{ cm}^2/\text{s}$ and a hydrodynamic radius of $R_H = 80 \text{ nm}$ are obtained. Using the second cumulant, a standard deviation of $\sigma = 1.03 \cdot 10^{-8} \text{ cm}^2/\text{s}$ was calculated. The particles increased in size and also the diffusion coefficient distribution became broader, which indicates aggregation over time.

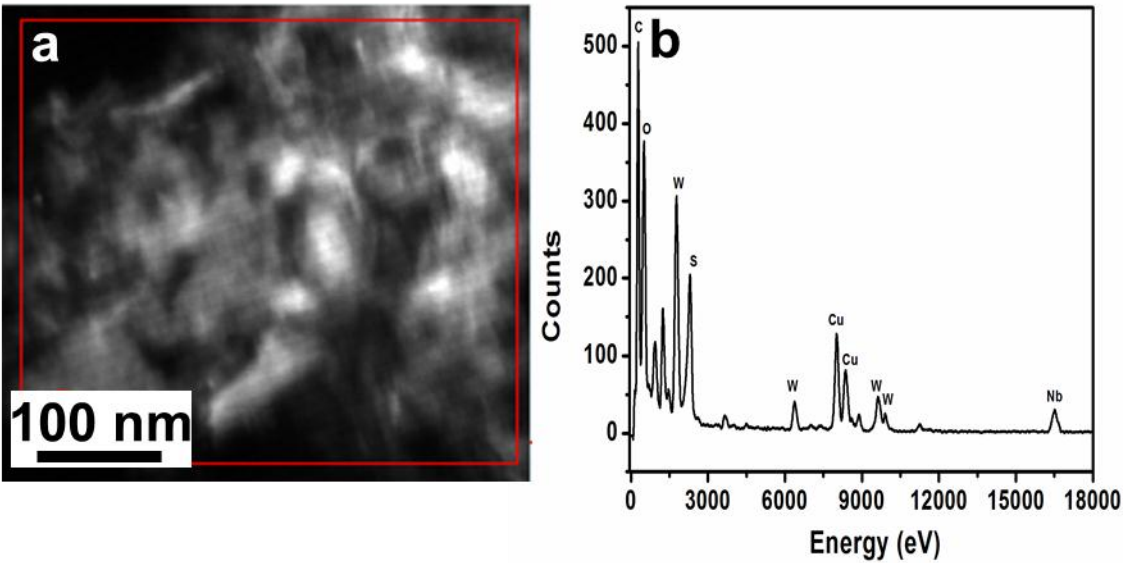


Fig. S1. (a) STEM image of the exfoliated coin rolls (b) EDX spectrum of the selected area.

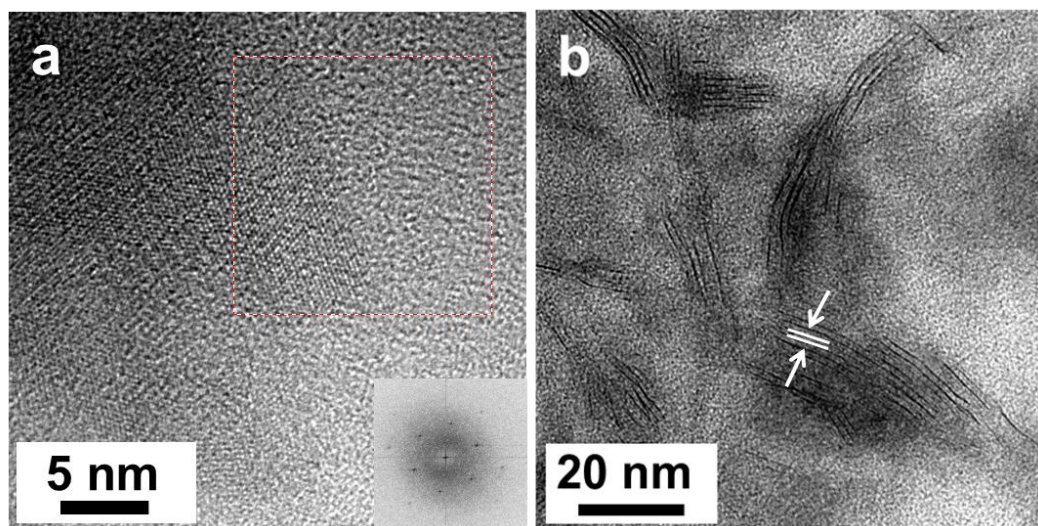


Fig. S2. (a) HRTEM image on the rim of a sheet (Inset: FFT on the selected area). (b) HRTEM image of few-layer sheets with an interlayer distance of $\sim 12\text{\AA}$.

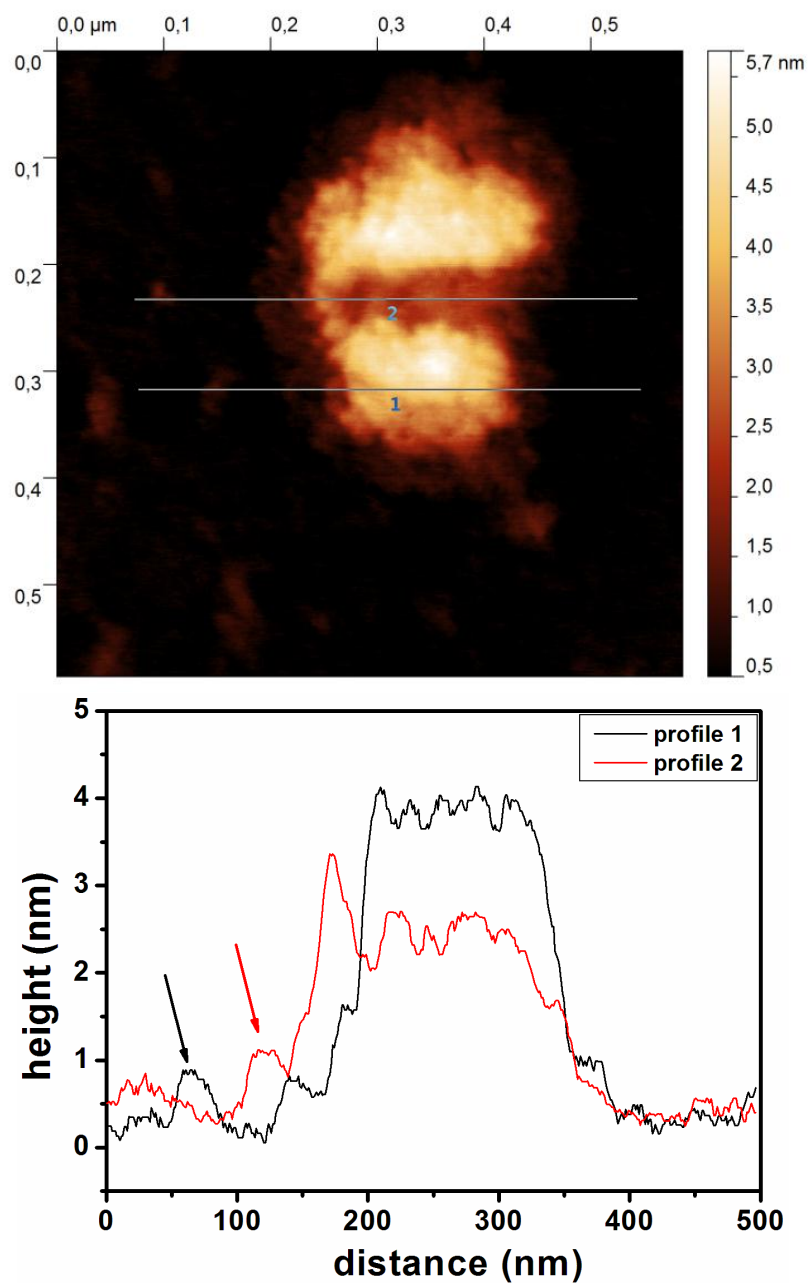


Fig. S3. SFM height image and corresponding profiles at various points to show the height of graphene-type sheets of $\text{Nb}_{1-x}\text{W}_x\text{S}_2$.

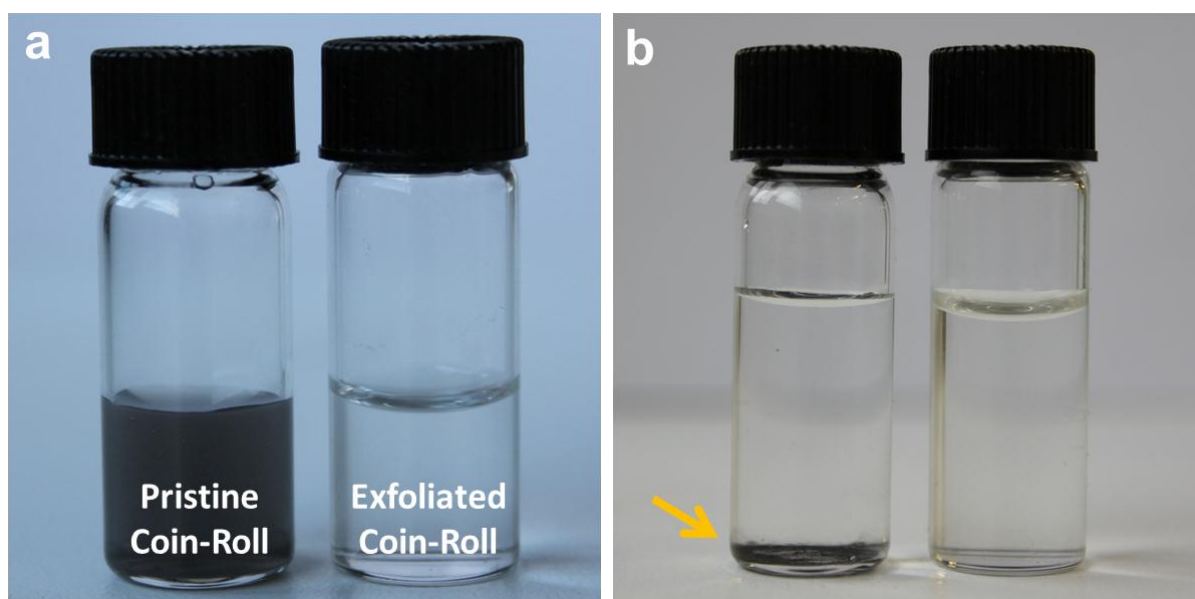


Fig. S4. (a) Digital micrograph of the coin-roll nanowires before (left) and after (right) exfoliation. (b) The same samples after 3 hours, showing the sedimentation of the dispersed pristine coin-roll nanowires.

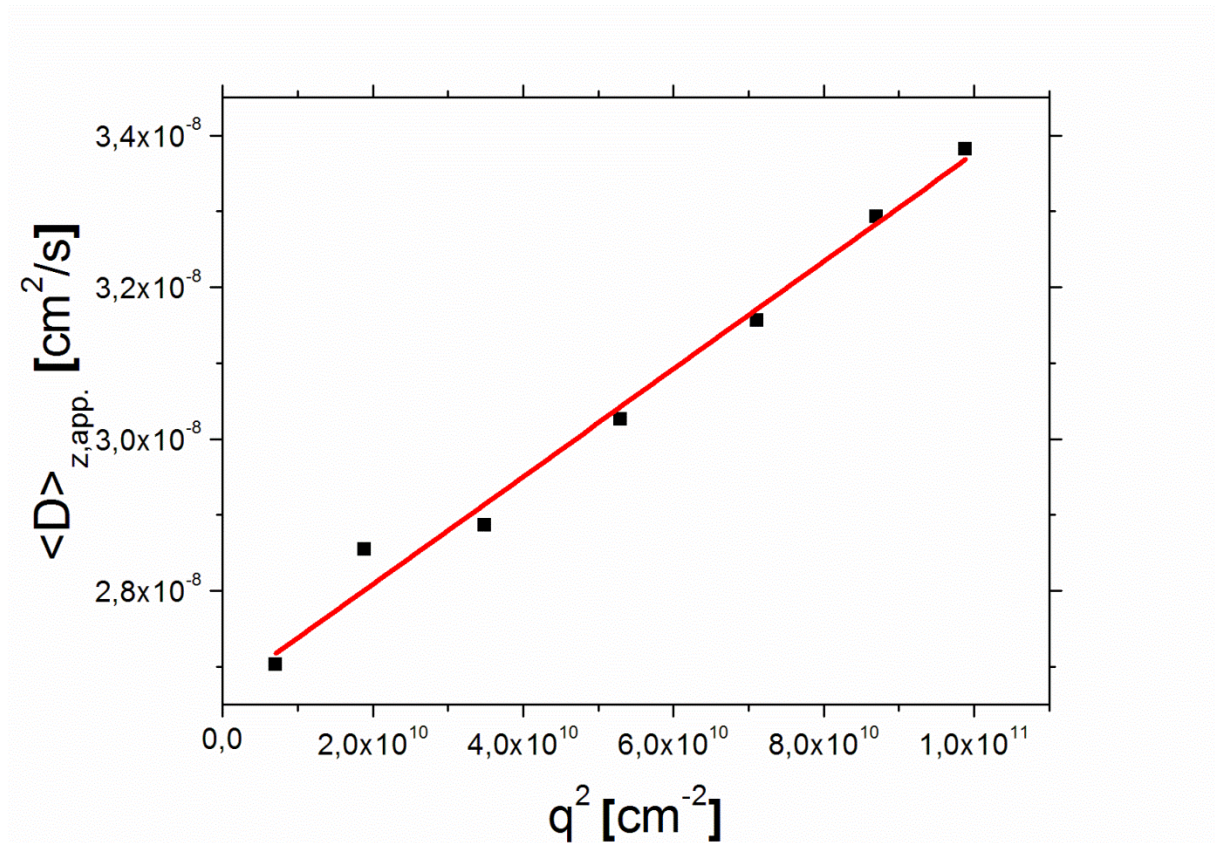


Fig. S5. Diffusion coefficients of the graphene-type sheets of Nb_{1-x}W_xS₂ recorded at different angles after 4 weeks.

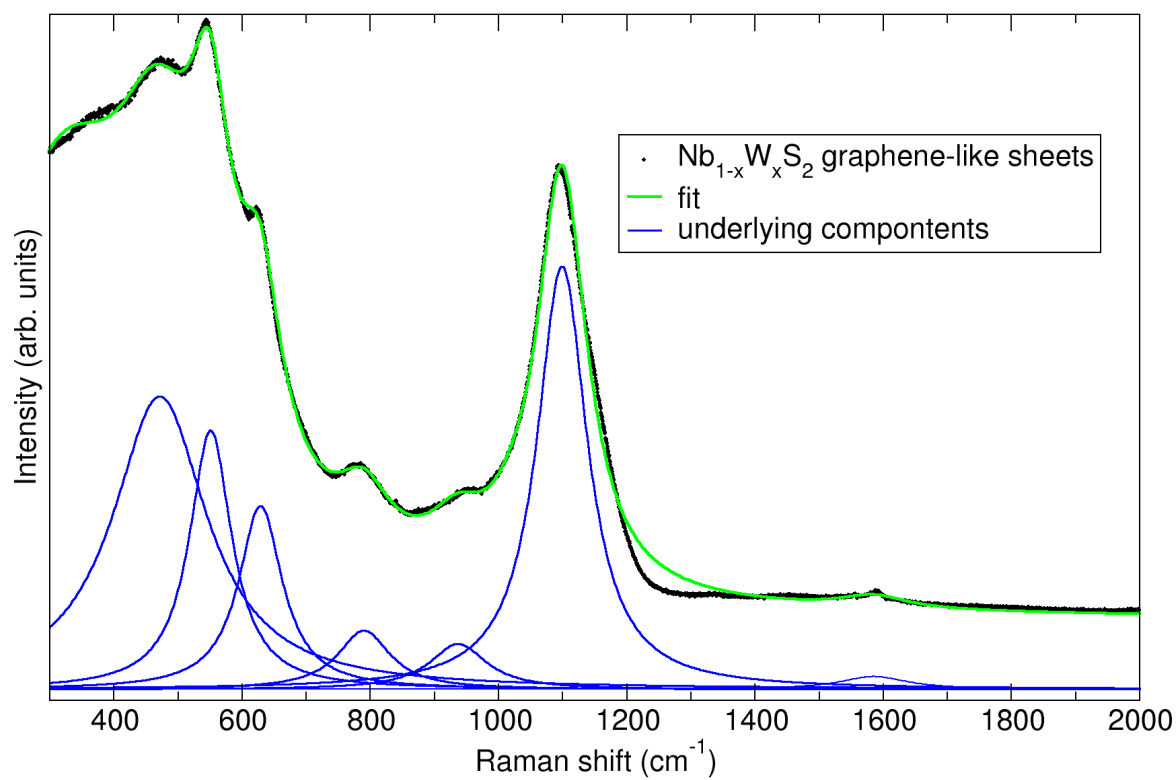


Fig. S6. Raman spectrum of exfoliated graphene-type sheets of $\text{Nb}_{1-x}\text{W}_x\text{S}_2$

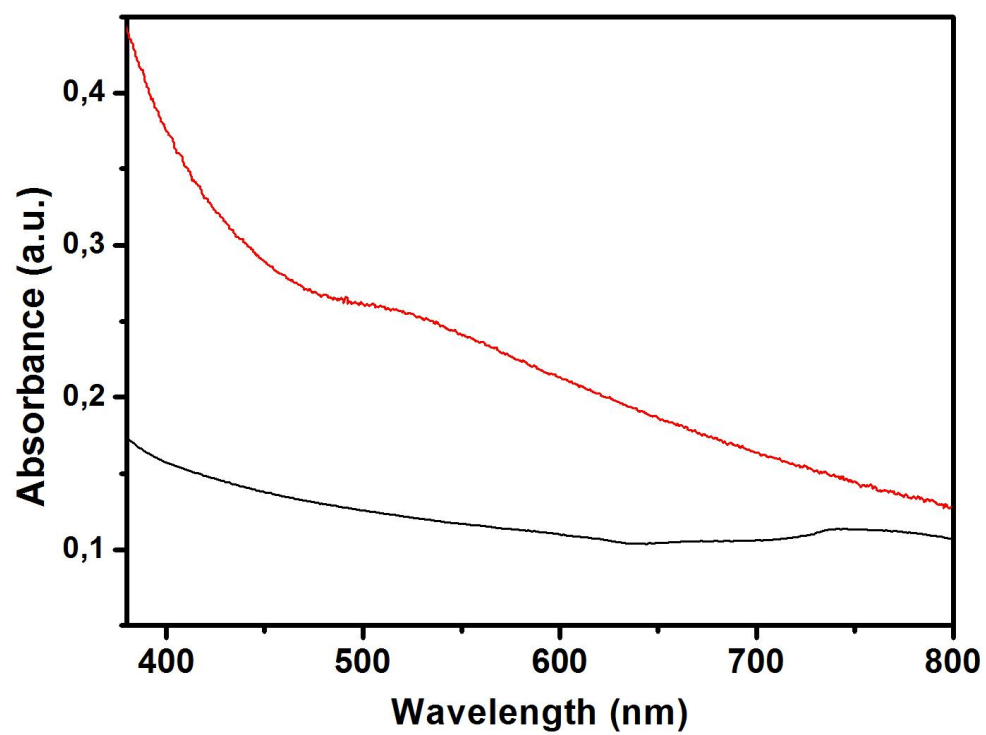


Fig. S7. UV/Vis absorption spectrum of: synthesized graphene-type sheets of Nb_{1-x}W_xS₂ (black line) Au nanoparticles functionalized (red line)

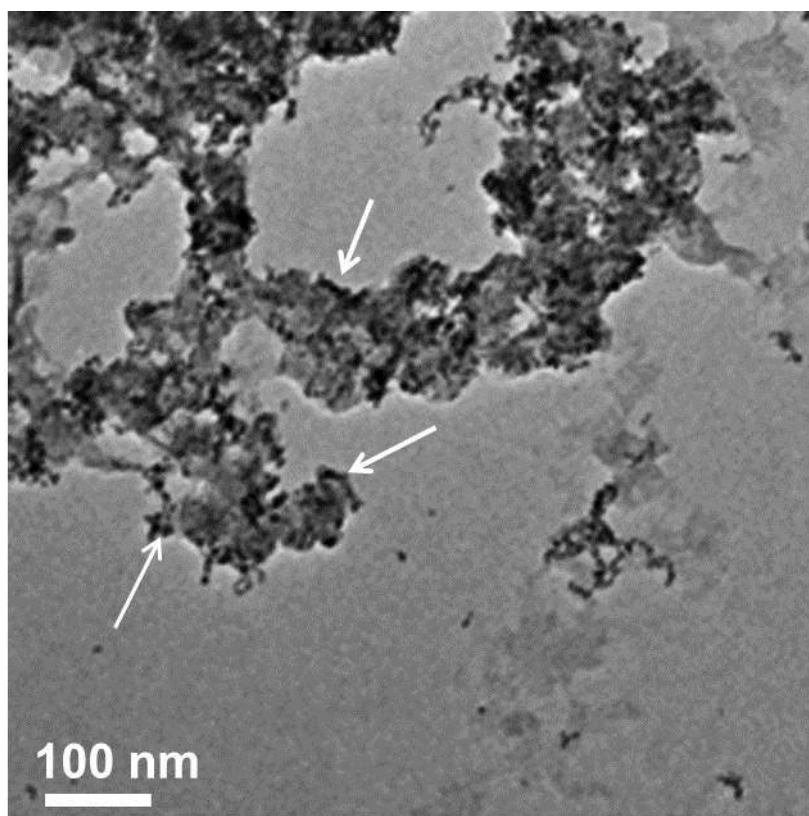


Fig. S8. TEM image showing the nucleation and growth of gold nanoparticles mostly edges of sheets as indicated by arrows.